JOURNAL OF PROPULSION AND POWER
Vol. 9, No. 1, Jan.–Feb. 1993

Experimental and Theoretical Study on Hollow-Cone Spray

Keh-Chin Chang,* Muh-Rong Wang,* Wen-Jing Wu,† and Chia-Hong Hong†
National Cheng-Kung University, Tainan 70101, Taiwan, Republic of China

A theoretical and experimental investigation has been conducted to study the two-phase turbulent structure in an isothermal hollow-cone spray. Mean and fluctuating velocity components, drop number density, as well as drop-size distribution were measured with a nonintrusive diagnostic tool, a two-component phase Doppler particle analyzer. Complete initial conditions required for theoretical calculations were also provided with measurements. Theoretical calculations were made with an Eulerian-Lagrangian formulism. Turbulent dispersion effects were numerically simulated using a Monte Carlo method. Turbulence modulation effects were also taken into account in the modeling. The well-defined experimental data were used to assess the accuracy of the resultant Eulerian-Lagrangian model. Comparisons showed that the theoretical predictions, based upon the Eulerian-Lagrangian model, yielded reasonable agreement with the experimental data. The improvements made by inclusion of the selected turbulence modulation model were insignificant in this work.

Nomenclature

b = spray half-width at the inlet station
C_D = drag coefficient
C_1, C_2, C_μ = coefficients in turbulent model
D = orifice diameter of spray nozzle
d_p = drop diameter
d_{32} = Sauter mean diameter
G = mean liquid mass flux
G_k = turbulence energy production term
g = gravity
k = turbulent kinetic energy
L_e = eddy size
M = total number of computational drops passing a cell
n = number of drops represented by a computational drop
P = value of probability density function
p = pressure
Re = drop Reynolds number
r = radial coordinate
$S_{p\phi}$ = source term due to interactions between gas and drops
S_ϕ = source term
t = time
U, u, u' = instantaneous, mean, and fluctuating axial velocity components
V, v, v' = instantaneous, mean, and fluctuating radial velocity components
V_c = cumulative volume fraction of liquid
w' = fluctuating tangential velocity component
x = axial coordinate
Γ_ϕ = transport coefficient
Δt = integrating time step
ε = dissipation rate of turbulent kinetic energy
μ, μ_t, μ_{eff} = molecular, eddy, effective viscosities
ρ = density
σ = coefficient in turbulent model
τ_e = turbulent eddy lifetime
τ_p = particle dynamic relaxation time
τ_r = residence time of particle in an eddy
ϕ = dependent variable
Ω = void fraction

Subscripts
i = ith direction
k = turbulent kinetic energy
p = dispersed phase
ε = dissipation rate of turbulent kinetic energy
$-$ = vector form

Superscripts
k = kth computational drop
$-$ = mean value

Received Dec. 17, 1991; revision received June 20, 1992; accepted for publication June 25, 1992.

*Associate Professor, Institute of Aeronautics and Astronautics. Member AIAA.
†Research Assistant.

I. Introduction

LIQUID fuel sprays have been extensively employed in combustion systems such as fuel-injected reciprocating engines, liquid rockets, gas turbine engines, etc. Since liquid-fuel sprays in combustion systems consist of several complicated processes—atomization, evaporation, mixing, and combustion—numerous efforts have been devoted to develop the theoretical methods and experimental instruments for analyzing these processes. Earlier studies have been reviewed in detail by Faeth[1,2] and Chigier.[3] Many recent experimental studies[4–9] were conducted to measure the spray angles, drop trajectories, drop velocities, and drop-size distributions. On the other hand, the current advances concerning the theoretical analysis of sprays and drop/turbulence interactions can be found in an excellent review paper by Faeth.[2] He pointed out that many fundamental problems such as the effects of anisotropic turbulence, turbulence modulation, turbulence dispersion, etc., remained to be resolved for dilute flows.

Quite a few theoretical studies[10–15] have revealed the importance of the inlet conditions of sprays on the prediction accuracy of the mixing, evaporation, and combustion characteristics. For example, Mellor et al.[16] conducted a hollow-cone spray experiment but provided incomplete measurements of the inlet conditions. Sturgess et al.[12] made many efforts to adjust the specification of the assumed inlet conditions in order to yield reasonable downstream spray predictions in their calculations. However, they confessed that, even with an artificial adjustment of the specification of the assumed inlet conditions required for theoretical calculations, they had never come to acceptable predictions of droplet space distribution. Asheim et al.[14] employed the same data base[16] and repeated the calculation but took into account the effects of droplet collisions. Little improvement of spray predictions, as compared to the measurements, was obtained

since the spray was of dilute case. Again, the prediction errors stemming from the incompletely measured inlet conditions remained in their theoretical analysis.

According to the preceding discussion, most of the experimental investigations did not provide complete measured information of inlet conditions due to the difficulty in measuring the inlet conditions of the dispersed phase. Consequently, it resulted in the limitation on the development of physical models and the numerical solution procedure. For example, in the absence of available inlet conditions, particularly for the dispersed phase, many theoretical investigations assumed the inlet profiles of radial velocity components of drops as a very rough function of spray angle[10,11,14,17] or even assumed the inlet radial velocity component to be zero for reasons of simplicity.[13] The size distribution of drops at the inlet was usually assumed in the Rosin-Rammler form and without spatial variation for the calculations.[10,12,14,17] In order to be rid of prediction uncertainties stemming from the lack of measured information at the inlet in the theoretical study of hollow-cone sprays, it is necessary to have available complete experimental data useful for the calculation of turbulent, polydisperse spray models. The present investigation using a relatively new instrument—a phase Doppler particle analyzer (PDPA)—differs from previous ones in many details, but principally in providing as complete information as possible about the mean and fluctuating properties for both continuous and dispersed phases in an isothermal hollow-cone spray.

In summary, the objectives of this study are twofold. The first one is to provide a well-defined, complete bench mark quality data base useful for model validation. The second one is to evaluate the theoretical calculations against the measurements in an isothermal hollow-cone spray which possesses elliptical characteristics in its corresponding mathematical formulism.

II. Experimental Methods

A. Test Facility

Figure 1a shows a schematic of the experimental setup which consists of a test stand as well as the air and fuel supply system. The test stand was composed of an optical table, a fuel collection tank, and exhaust system, and a three-axis transverse mechanism which permits positioning to within 0.03 mm. The spray nozzle was mounted on the three-axis transverse mechanism and was positioned by stepping motors that were controlled by a PC/XT. The exhaust system provided a uniform curtain flow of the surrounding air with a velocity of 0.5 m/s in the test section to avoid the flow reversal. The test chamber cross section was 0.8 × 0.8 m with a length of 0.7 m. The spray nozzle was a pressure type of hollow-cone atomizer (Monarch model F80 no. 1.35, as schematically shown in Fig. 1b) from which the water spray was injected vertically downward with a flow rate of 1.19 g/s. The orifice diameter of the nozzle was 0.64 mm. The nominal cone angle was 80 deg. The water was maintained at room temperature (298 ± 2 K), and the experiment was conducted at a pressure difference across the atomizer of 827 kPa (120 psi). Since the spray was axisymmetric, a two-dimensional, cylindrical coordinate was selected such that the axial (x) coordinate (along the axis) is positive downward with the origin at the center of the nozzle exit and the radial (r) coordinate (normal to the axis) is positive away from the axis.

B. Instrumentation

Mean and fluctuating velocities of both phases were measured with a two-component PDPA (Aerometric, Inc., model 3200-3). This instrument can simultaneously measure two orthogonal components of velocity, volume flux, and size for individual drops.[18] A smoke generator (using kerosene as the working fluid) was used to generate seeding particles (nominal 2 μm) for the velocity measurements of the continuous phase. The ensemble-averaged quantities were statistically calculated

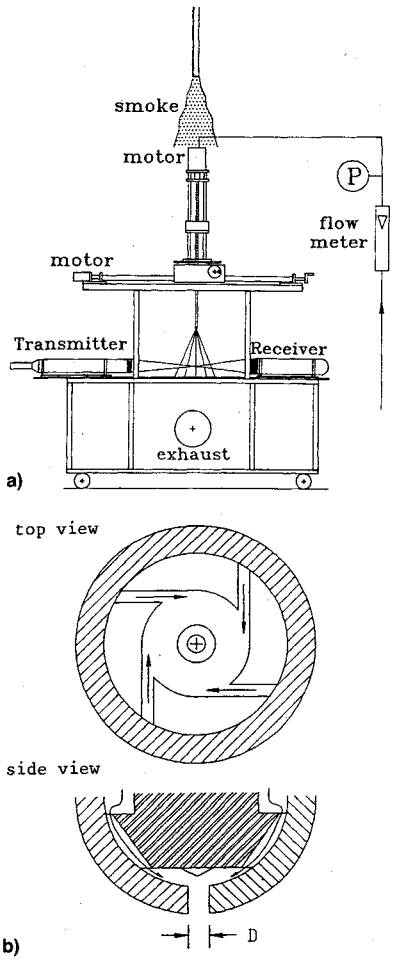

Fig. 1 Schematics of a) the test facility, and b) the internal configuration of the nozzle.

by collecting 30,000 valid sample data for each measurement point. Typically, a drop number density of 10^4 drops/cc was measured in the central regions of the spray, except in the dilute outer regions of the spray where the drop number density dropped to about 1.5×10^2 drops/cc. It was found that the measurement of the volume flux was sensitive to the PDPA's settings. The proper settings of the range of the laser power, the PMT voltage size range, the optical arrangement, etc. in the experiment were determined by assuring the repeatability of the measured data and the good conservation of the liquid-mass flow rate at all measured axial stations. Moreover, the size distribution range injected by the spray nozzle was able to be covered by one optical arrangement without changing the track number of the grating disk of the PDPA. The accuracy of the measured volume flux was about 75 ~ 85% as compared with the metered mass flow rate. More details of the experimental methods can be found in Ref. 19.

Ten data sets with the mean drop sizes of 7, 21, 35, 49, 63, 77, 91, 105, 119, and 133 μm were recorded in the experiment. The complete information including the distributions of u, v, u', v', w', $\overline{u'v'}$, u_p^k, v_p^k, G_p^k, and drop size measured at the axial station of $x/D = 20$ will serve as the inlet conditions required for the theoretical calculation. Although the liquid was swirled prior to injection in accordance with the nozzle geometry (see Fig. 1b), the swirling motion was relatively weak and almost zero values of the measured mean azimuthal velocity component for both phases were observed at the axial station of $x/D = 20$. Thus, the present problem can be viewed as a nonswirling spray.

III. Theoretical Methods

In general, there are two fundamentally different theoretical approaches utilized to predict the dispersed properties in

two-phase flow.[2,20] One is called the Eulerian approach or two-fluid model, the other is called the Lagrangian or tracking approach. Durst[21] examined these two different approaches and showed that the Lagrangian approach had an advantage in handling dilute flows with polydisperse size distributions, whereas the Eulerian approach was relatively computationally efficient for monodisperse two-phase flows. The comparative studies using these two approaches conducted by Mostafa and Mongia[22] as well as Adeniji-Fashola and Chen[23] also came to similar conclusions. Since the problem to be addressed is a polydisperse spray, the Lagrangian approach is employed for the theoretical analysis of the dispersed phase.

A. Continuous Phase Equations

The k-ε turbulence model capable of adeequately describing the turbulence motion of simple flows such as the present nonswirling spray is employed in this work. The governing equations of the continuous phase consist of the conservation of mass and momentum in conjunction with the turbulence modeling equations for turbulent kinetic energy and its dissipation rate. The governing equations expressed in the Reynold-averaged form for the axisymmetric cylindrical coordinate are cast into a general form which permits a single algorithm to be used for calculation, as follows:

$$\frac{\partial}{\partial x}(\rho\Omega u\phi) + \frac{1}{r}\frac{\partial}{\partial r}(r\rho\Omega v\phi) = \frac{\partial}{\partial x}\left(\Omega\Gamma_\phi\frac{\partial\phi}{\partial x}\right) + \frac{1}{r}\frac{\partial}{\partial r}\left(r\Omega\Gamma_\phi\frac{\partial\phi}{\partial r}\right) + S_\phi + S_{p\phi} \quad (1)$$

The parameters ϕ, Γ_ϕ, S_ϕ, and $S_{p\phi}$ appearing in Eq. (1) are summarized in Table 1, along with the appropriate empirical constants.[24] Here $S_{p\phi}$ represents the source term due to the interactions between the continuous and dispersed phases. The calculated values of Ω range between 0.9999–1.0 in the present case. Therefore, the investigated spray is not a dense two-phase flow and the drop-drop interactions can be reasonably ignored in the modeling.

It is known[2,25] that the effects of the dispersed phase on the continuous phase are not only through the production of momentum source terms but also through the modification of turbulence structure. However, the effects of turbulence modulation due to the existence of dispersed phase were seldom considered in most of the previous theoretical investigations[10–15,17] since those sprays were of dilute two-phase cases. In this study the effects of turbulence modulation are also examined by employing the model developed by Shuen et al.[26] as shown in the following:

$$S_{pk} = \Omega\overline{US_{pu}} + \Omega\overline{VS_{pv}} - \Omega u\overline{S_{pu}} - \Omega v\overline{S_{pu}} \quad (2)$$

$$S_{p\varepsilon} = -C_3\rho\frac{\varepsilon}{k}(\overline{u'S'_{pu}} + \overline{v'S'_{pv}}) \quad (3)$$

with $C_3 = 1.5$.

B. Dispersed Phase Equations

The dispersed phase is treated by tracking individual drops as they move through the turbulence field of the continuous phase (Lagrangian approach). This is essentially a statistical (Monte Carlo) approach and requires the tracking of an adequate number of computational drops in order to obtain statistically stationary information for the dispersed phase. Each of these computational drops characterizes a group of physical drops possessing the same size and velocity.

The equation of motion for the kth computational drop was originally derived by Basset, Bonssinesq, and Oseen, and is known as the B—B—O equation.[27] For large drop-to-gas density ratios ($\rho_p/\rho \simeq 900$ in this work), effects of static pressure gradients, virtual mass; Basset, and Magnus forces can be neglected with little errors. Associated with the previously stated assumptions, the position and velocity of the kth computational drop in the ith direction becomes

$$\frac{dx^k_{pi}}{dt} = U^k_{pi} \quad (4)$$

$$\frac{dU^k_{pi}}{dt} = \frac{U_i - U^k_{pi}}{\tau^k_p} + g_i \quad (5)$$

where

$$\tau^k_p = \frac{4d^k_p\rho_p}{3C^k_D\rho|\underline{U} - \underline{U^k_p}|} \quad (6)$$

$$U_i = u_i + u'_i \quad (7)$$

Note that the velocities (U_i) shown in the above equations denote instantaneous velocities. The drag coefficient for a

Table 1 Governing equations of the continuous phase

ϕ	Γ_ϕ	S_ϕ	$S_{p\phi}$
1	0	0	0
u	μ_{eff}	$-\Omega\frac{\partial p}{\partial x} + \frac{\partial}{\partial x}\left(\Omega\mu_{\text{eff}}\frac{\partial u}{\partial x}\right) + \frac{1}{r}\frac{\partial}{\partial r}\left(r\Omega\mu_{\text{eff}}\frac{\partial v}{\partial x}\right)$	S_{pu}
v	μ_{eff}	$-\Omega\frac{\partial p}{\partial r} - 2\Omega\mu_{\text{eff}}\frac{v}{r^2} + \frac{\partial}{\partial x}\left(\Omega\mu_{\text{eff}}\frac{\partial u}{\partial r}\right) + \frac{1}{r}\frac{\partial}{\partial r}\left(r\Omega\mu_{\text{eff}}\frac{\partial v}{\partial r}\right)$	S_{pv}
k	$\mu_{\text{eff}}/\sigma_k$	$\Omega(G_k - \rho\varepsilon)$	S_{pk}
ε	$\mu_{\text{eff}}/\sigma_\varepsilon$	$\Omega(C_1G_k - C_2\rho\varepsilon)\frac{\varepsilon}{k}$	$S_{p\varepsilon}$

$$G_k = \mu_t\left\{2\left[\left(\frac{\partial u}{\partial x}\right)^2 + \left(\frac{\partial v}{\partial r}\right)^2 + \left(\frac{v}{r}\right)^2\right] + \left(\frac{\partial v}{\partial x} + \frac{\partial u}{\partial r}\right)^2\right\}$$

$$\mu_t = C_\mu\rho k^2/\varepsilon, \qquad \mu_{\text{eff}} = \mu + \mu_t$$

$C\mu$	C_1	C_2	σ_k	σ_ε
0.09	1.44	1.87	1.0	1.3

S_{pu} and S_{pv} are obtained with the PSI—cell method. S_{pk} and $S_{p\varepsilon}$ are obtained from Eqs. (2) and (3).

spherical drop is given by an empirical formula[28]

$$C_D^k = \frac{24}{Re^k}\left[1 + \frac{(Re^k)^{2/3}}{6}\right], \quad Re^k \le 1000$$
$$= 0.44, \quad Re^k > 1000 \tag{8}$$

where the drop Reynolds number is defined by

$$Re^k = \rho|\underline{U} - \underline{U}_p^k|\mathrm{d}_p^k/\mu \tag{9}$$

The trajectory of the kth computational drop is determined by directly integrating its velocity with respect to time.

Drops are assumed to interact with an eddy in the turbulent field for a time which is determined as the smaller of the eddy lifetime (τ_e) and the residence time of the kth computational drop in the eddy (τ_r^k). Hence, to ensure the drop-eddy interaction Δt must satisfy the following criteria:

$$\Delta t \le \min(\tau_e, \tau_r^k) \tag{10}$$

If the characteristic size of an eddy is assumed to be its dissipation scale L_e given by

$$L_e = C_\mu^{3/4} k^{3/2}/\varepsilon \tag{11}$$

the eddy lifetime is then estimated as[26]

$$\tau_e = L_e/|\underline{u}'| \tag{12}$$

The residence time of the kth computational drop in the eddy is obtained from

$$\tau_r = L_e/|\underline{U} - \underline{U}_p^k| \tag{13}$$

IV. Numerical Solution Procedure

Equation (1) possesses mathematically elliptic characteristics and is solved using the finite-volume method in association with the SIMPLER algorithm and the power-law scheme.[29] The computational domain is bounded from $x/D = 20$ to $x/D = 150$ and from the axis of symmetry to $r/D = 150$ along the axial and radial direction, respectively. A nonuniform grid mesh composed of 35 × 42 (axial by radial coordinates) nodes. Distribution of grid nodes is arranged to ensure that small regions exerting a large influence on the flowfield are sufficiently resolved.

Consistent with the use of the k-ε model for the continuous phase, the fluctuating velocity u_i' is assumed to be an isotropic Gaussian function having the standard deviation of $\sqrt{\frac{2}{3}k}$. Hence, for a given u_i' at each integrating time step Δt, there exists a corresponding value of probability density function, e.g., P. In order to obtain a statistically stationary solution, 10 groups of different drop diameters, each being divided into 600 computational drops, are employed in the calculations.

The instantaneous velocity components of the dispersed phase are determined by iteratively intergrating the nonlinear ordinary differential equation of Eq. (5) to an acceptable tolerance in a given time step. The mean value of the dispersed-phase velocity at a specified grid node is calculated by use of the ensemble averaging concept

$$u_{pi} = \sum_{m=1}^{M} n_m P_m U_{pi}^m \Big/ \sum_{m=1}^{M} n_m P_m \tag{14}$$

where the index m denotes the mth computational group passing through the crossing surface normal to the direction i at a specified grid node.

The source terms due to two-phase interactions S_{pu} and S_{pv} in the continuous-phase momentum equations (see Table 1) are obtained using the PSI-cell method suggested by Crowe et al.[30] The criterion based upon the normalized momentum residual is set to be 10^{-5} for monitoring convergence of all continuous-phase governing equations.

A. Boundary Conditions

At the inlet station of $x/D = 20$ all the required information except ε is specified using the measured data. However, the required ε information at the inlet station can be obtained by combining the Boussinesq hypothesis for the shear stress and the relationship of the eddy viscosity between k and ε. The shear stress $\overline{u'v'}$ measured at the inlet station is expressed by

$$-\rho\overline{u'v'} = \mu_t\left(\frac{\partial u}{\partial r} + \frac{\partial v}{\partial x}\right) \tag{15}$$

However, the measured results presented in Fig. 2 revealed that $\partial v/\partial x << \partial u/\partial r$ in the region near the inlet station. Association with this observation and introduction of the definition of the eddy viscosity (see Table 1) into Eq. (15) yields

$$\varepsilon = -C_\mu k^2 \frac{\partial u}{\partial r} \Big/ \overline{u'v'} \tag{16}$$

The inlet ε information can then be calculated using the measured u, k, and $\overline{u'v'}$ in the experiment. It is noted that the calculated ε profile can be approximately expressed in the following form by the best comparison with the prediction of Eq. (16)

$$\varepsilon = C_\mu k^{3/2}/(0.045b) \tag{17}$$

where b denotes the half-width of the spray at $x/D = 20$ and is equal to 32 D from the PDPA measurements.

For the axis of symmetry, the gradient type boundary condition $\partial\phi/\partial r = 0$ is made except for the radial velocity component which is itself zero. The entrainment boundary condition is represented by $\partial\phi/\partial r = 0$ at a sufficiently far lateral distance. The outlet boundary condition is assumed to be a fully developed type, i.e., $\partial\phi/\partial x = 0$. Predictions were made with different lateral and axial lengths for the computational domain. The results reveal that the presently employed lateral length (150 D) and axial length (130 D) adequately ensure the validity of the assumed entrainment and outlet boundary conditions.

V. Results and Discussion

Both predictions obtained with and without inclusion of the turbulence modulation model developed by Shuen et al.[26] are presented and compared to the measurements in this work. Note that in order to discriminate the differences between these two predictions (with and without turbulence modulation effects), the scales of the mean properties have been purposely enlarged in the last two axial stations ($x/D = 80$ and 130) in some figures of this work.

The evolution of the predicted and measured mean axial and radial velocity components of the continuous phase is plotted in Fig. 2. As observed from Fig. 2b, the negative values of mean radial velocity component in the outer lateral regions indicate entrainment of the ambient air to the spray. However, the momentum transferred from the dispersed phase (see Fig. 5) by way of aerodynamic drag results in changes of mean radial velocity component from negative to positive values in some inner lateral positions as exhibited in Fig. 2b. Comparisons between the measurements and both predictions of velocity with and without the turbulence modulation model show that slight improvements are obtained in the downstream regions by taking into consideration the turbulence modulation effects in the theoretical analysis.

The evolution of the predicted and measured turbulent kinetic energy of the continuous phase is plotted in Fig. 3. Clearly, the values of turbulent kinetic energy are overpredicted in the core regions although the inclusion of the tur-

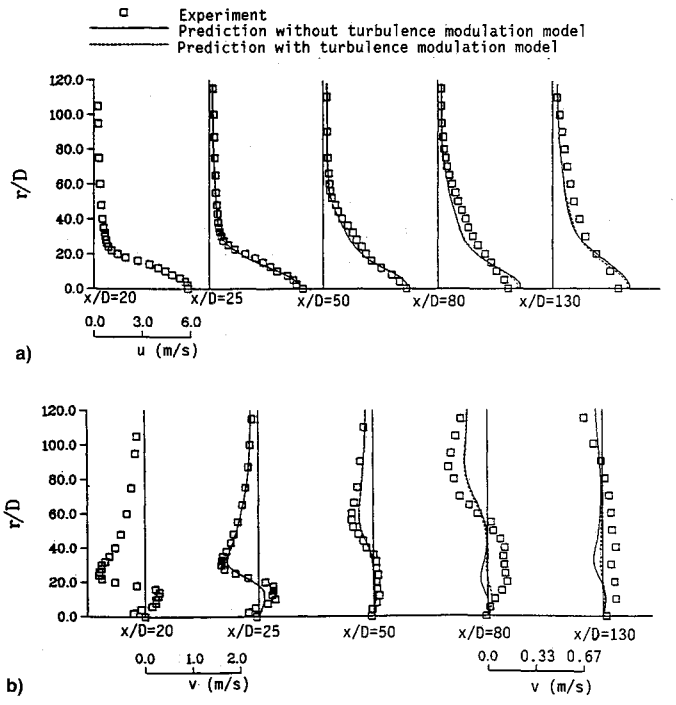

Fig. 2 Evolution of the predicted and measured a) mean axial velocity components, and b) mean radial velocity components of the continuous phase.

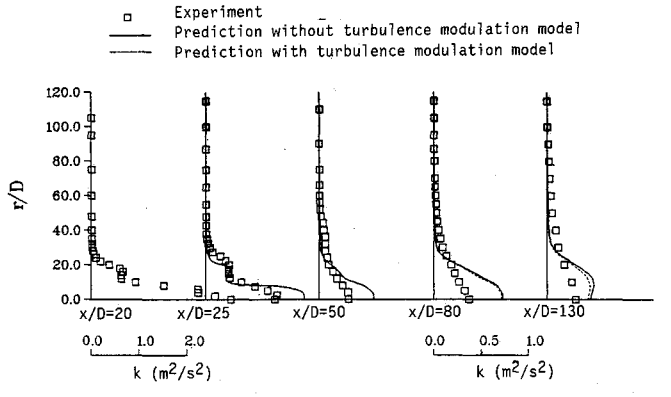

Fig. 3 Evolution of the predicted and measured turbulent kinetic energy of the continuous phase.

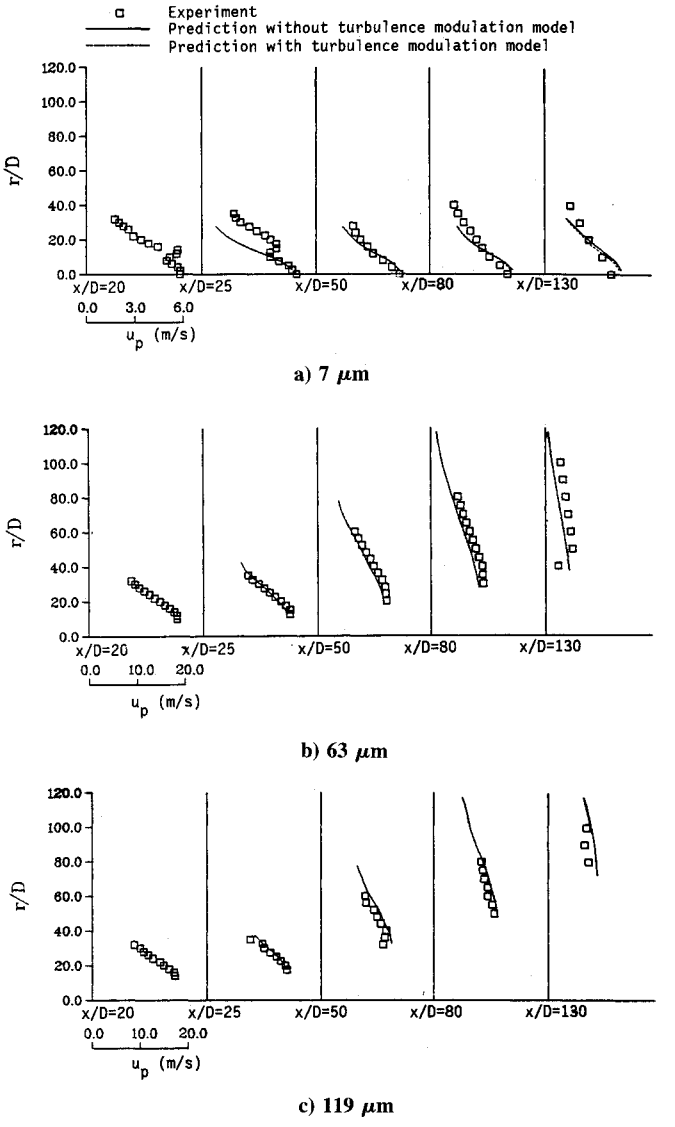

Fig. 4 Evolution of the predicted and measured mean axial velocity components of the drops.

bulence modulation model can alleviate, to a slight extent, overpredictions in the downstream regions. In the present modeling work there are two possible reasons for these descrepancies between the predictions and the measurements. One is the suitability of the isotropic k-ε turbulence model applicable to the present two-phase hollow-cone flowfield. The other is the reliability of the turbulence modulation model which was developed by Shuen et al.[26] and has not been subjected to stringent validation so far. However, this issue remains to be investigated further.

As stated in Sec. II, 10 discrete drop sizes were employed in this work to simulate the spectral effects of the size distribution in the spray. For the sake of abbreviation only the results with the sizes of 7, 63, and 119 μm representing small, medium, and large drops are reported here. Other inlet conditions of the dispersed phase for the remaining discrete drop sizes required for theoretical calculations can be found in Ref. 19.

The evolution of the predicted and measured mean axial and radial velocity components with these three drop sizes is plotted in Figs. 4 and 5, respectively. Agreements between the predictions and measurements are generally good except for the case of $d_p = 7$ μm. Similar unsatisfactory agreements are also observed for the cases of other small drops such as $d_p = 21$ and 35 μm which are not presented here for the sake of abbreviation. Small drops which have large surface-to-volume ratios are known to reach locally dynamic equilibrium with the continuous phase more quickly than large drops. The predicted results of the smallest drops ($d_p = 7$ μm) shown in Figs. 4a and 5a do exhibit this trend as compared to the continuous-phase results (Fig. 2). Nevertheless, comparisons between the measured drop velocities of $d_p = 7$ μm (Figs. 4a and 5a) and the measured gas velocities (Figs. 2a and 2b) show that there exist some drops with $d_p = 7$ μm having significantly higher velocities than the continuous phase. Based upon the observations from the evolution of drop-size spectrum and the Weber number along the axial distance, Hong[19] argued that these small drops having higher velocities than the gas might be broken up due to drop collisions from the larger drops, which have much higher velocities than the small drops (cf. Figs. 4 and 5) in a secondary atomization process which was different from the primary atomization process that occurred in the neighborhood of the spray-nozzle exit.

One may raise a question as to whether the present theoretical model (which excluded the break-up process) can adequately represent the physical phenomena that occurred in the investigated hollow-cone spray. To answer this question the evolution of the predicted and measured mean liquid mass

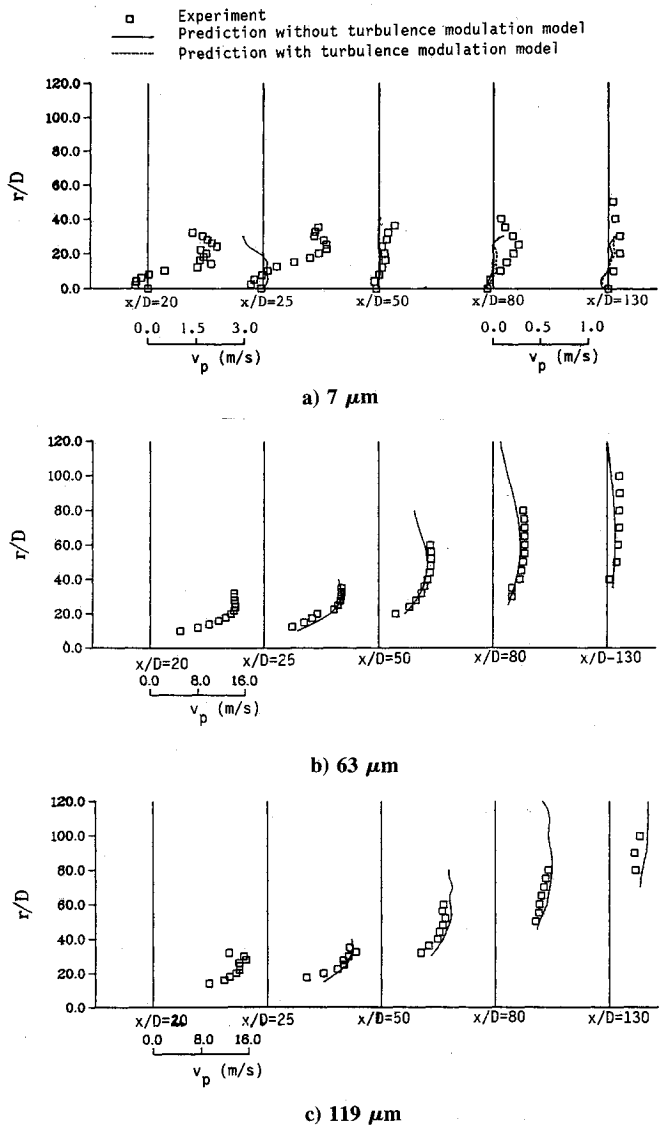

Fig. 5 Evolution of the predicted and measured mean radial velocity components of the drops.

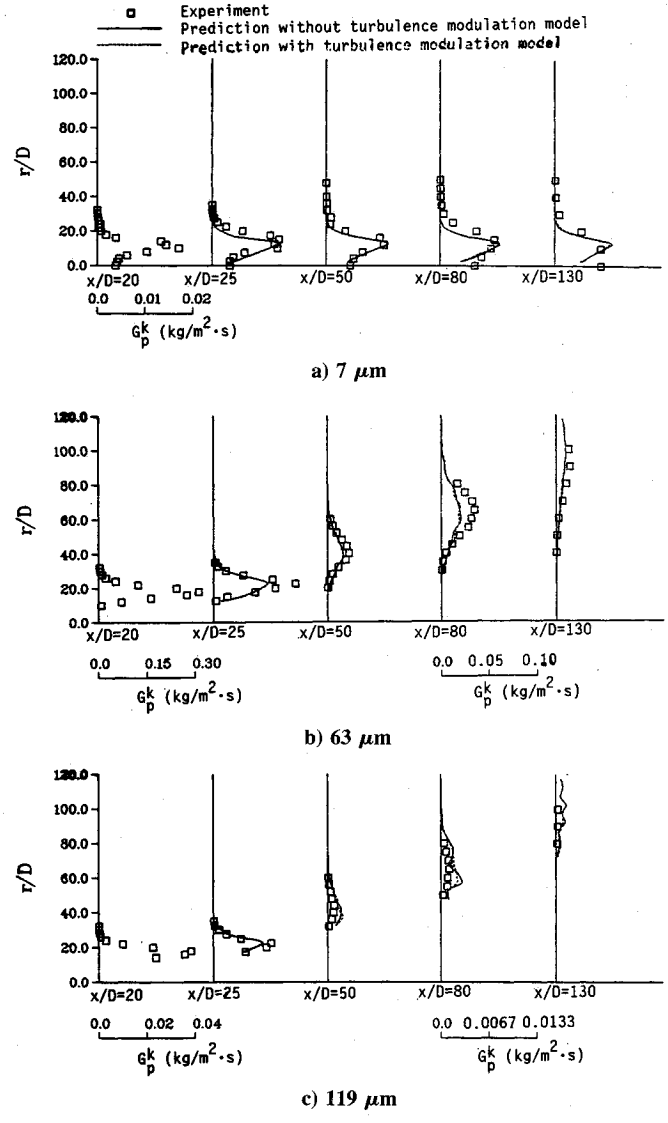

Fig. 6 Evolution of the predicted and measured liquid mass fluxes.

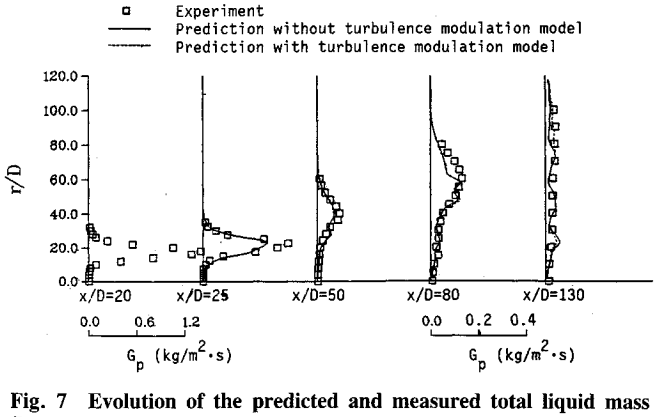

Fig. 7 Evolution of the predicted and measured total liquid mass fluxes.

fluxes with these three different sizes is plotted and compared in Fig. 6. Special attention is paid to the results with $d_p = 7$ μm at $x/D = 25$ (see Fig. 6a). At first there are no apparent jumping data such as u_p shown in Fig. 4a, appearing in the measurements of G_p^k. Secondly, agreement between the predictions and measurements at this axial station is quite satisfactory. These observations imply that the number of drops with $d_p = 7$ μm, which were broken up from large drops having higher velocities, is few in comparison with the number of other drops with $d_p = 7$ μm conveyed from the neighboring control volumes. As a result, the neglect of the drop breakup process in the model does not introduce significant errors in the present spray prediction. The results shown in Fig. 6 indicate a trend that the larger drops move along with their original flight angles and can then penetrate to the outer lateral regions of the spray. On the other hand, the smaller drops are mostly confined in the core regions of the spray.

Figure 7 presents the evolution of the predicted and measured mean total liquid mass fluxes. As revealed from this figure, the distribution of the mean total liquid mass flux becomes more evenly distributed as the axial distance increases. However, from the previous discussion, the sectional distribution of mean drop size can never become as even as that of mean total liquid mass flux in the downstream of the spray. This is shown by checking the evolution of the Sauter mean diameter of drops given in Fig. 8. Clearly, the spray shows an uneven distribution of drop sizes in the investigated flowfield. As expected, the larger the drop size is the more outer lateral position it can reach. Agreement between the predictions and measurements shown in Fig. 8 further implies that the present employment of 10 discrete drop sizes can adequately represent the size-spectal effects in the simulation.

In general, the theoretical predictions of the dispersed phase are in good agreement with the measurements. Also, the improvements of predictions made by consideration of the turbulence modulation effects are negligibly small. This is

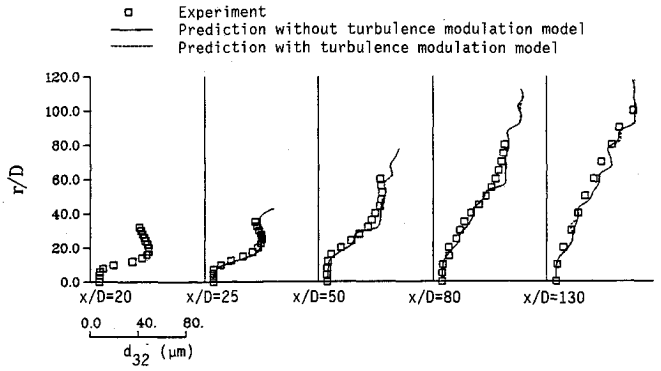

Fig. 8 Evolution of the predicted and measured Sauter mean diameters of the drops.

because the employed turbulence modulation model did not lead to any significant changes in the predictions of the continuous phase.

VI. Conclusions

A detailed well-defined data set useful for model validation in an isothermal hollow-cone spray is presented. Complete initial conditions required for theoretical calculations were provided with measurements to avoid prediction uncertainty introduced from the usual assumptions of initial conditions.

The theoretical investigation is performed with the Eulerian-Lagrangian formulism. The flow properties of the dispersed phase are calculated using the Monte Carlo method. The accuracy of the theoretical predictions of a two-phase structure has been well-assessed by the measured data. The employed turbulence modulation model is found to have only slight improvements on the continuous-phase predictions and, consequently, leads to negligibly small influences on the predictions of the dispersed-phase properties. Some peculiar velocity data appearing in the PDPA measurements of small drops are also discussed and are attributed to a secondary atomization process of the spray.

Acknowledgment

This work was sponsored by the National Science Council of the Republic of China under contract NSC 80-0210-D006-27.

References

[1]Faeth, G. M., "Evaporation and Combustion of Sprays," *Progress in Energy and Combustion Science*, Vol. 9, No. 1, 1983, pp. 1–76.

[2]Faeth, G. M., "Mixing, Transport and Combustion in Sprays," *Progress in Energy and Combustion Science*, Vol. 13, No. 4, 1987, pp. 293–345.

[3]Chigier, N. A., "The Atomization and Burning of Liquid Fuel Spray," *Progress in Energy and Combustion Science*, Vol. 2, No. 2, 1976, pp. 97–114.

[4]Wu, K.-J., Su, C.-C., Steinberger, R. L., Santavicca, D. A., and Bracco, F. V, "Measurement of the Spray Angle of Atomizing Jets," *Transactions of the ASME Journal of Fluids Engineering*, Vol. 105, No. 4, 1983, pp. 406–413.

[5]Wu, K.-J., Santavicca, D. A., Bracco, F. V., and Coghe, A., "LDV Measurements of Drop Velocity in Diesel-Type Sprays," *AIAA Journal*, Vol. 22, No. 9, 1984, pp. 1263–1270.

[6]Bachalo, W. D., Houser, M. J., and Smith, J. N., "Evolutionary Behavior of Sprays Produced by Pressure Atomizers," AIAA Paper 86-0296, Reno, NV, Jan. 1986.

[7]Fulton, D., and Tankin, R. S., "Spray from a Bluff Body Combustor in Annular Air Flow," *Combustion Science and Technology*, Vol. 59, Nos. 1–3, 1988, pp. 1–26.

[8]Li, X., and Tankin, R. S., "Spray Behavior in Annular Air Streams," *Combustion Science and Technology*, Vol. 64, Nos. 1–3, 1989, pp. 141–165.

[9]McDonell, V. G., and Samuelsen, S., "Gas and Drop Behavior in Reacting and Non-Reacting Air-Blast Atomizer Sprays," *Journal of Propulsion and Power*, Vol. 7, No. 5, 1991, pp. 684–691.

[10]El Banhawy, Y., and Whitelaw, J. H., "Calculation of the Flow Properties of a Confined Kerosene-Spray Flame," *AIAA Journal*, Vol. 18, No. 12, 1980, pp. 1503–1510.

[11]Gosman, A. D., and Ioannides, E., "Aspects of Computer Simulation of Liquid-Fuelled Combustors," AIAA Paper 81-0323, St. Louis, MO, Jan. 1981.

[12]Sturgess, G. J., Syed, S. A., and McManus, K. R., "Calculation of a Hollow-Cone Liquid Spray in a Uniform Airstream," *Journal of Propulsion and Power*, Vol. 1, No. 5, 1985, pp. 360–369.

[13]Kirwan, J. E., Lee, T. A., Schroering, G. N., Peters, J. E., Renie, J. P., and Kim, K., "Experimental and Theoretical Study of a Monodisperse Spray," *Journal of Propulsion and Power*, Vol. 4, No. 4, 1988, pp. 299–307.

[14]Asheim, J. P., Kirwan, J. E., and Peters, J. E., "Modeling of a Hollow-Cone Liquid Spray Including Droplet Collisions," *Journal of Propulsion and Power*, Vol. 4, No. 5, 1988, pp. 391–398.

[15]Dodge, L. G., and Schwalb, J. A., "Fuel Spray Evolution: Comparison of Experiment and CFD Simulation of Nonevaporating Spray," *Transactions of the ASME Journal of Engineering for Gas Turbines and Power*, Vol. 111, No. 1, 1989, pp. 15–23.

[16]Mellor, R., Chigier, N. A., and Beer, J. M., "Hollow-Cone Liquid Spray in Uniform Air Stream," *Proceedings of the Symposium on Combusiton and Heat Transfer in Gas Turbine Systems*, edited by E. R. Noster, Cranfield International Symposium Series, Vol. 11, Pergamon, Oxford, England, UK, 1971, pp. 291–305.

[17]Boysan, F., Ayers, W. H., Swithenbank, J., and Pan, Z., "Three-Dimensional Model of Spray Combustion in Gas Turbine Combustors," *Journal of Energy*, Vol. 6, No. 6, 1982, pp. 368–375.

[18]Bachalo, W. D., and Houser, M. J., "Phase Doppler Spray Analyzer for Simultaneous Measurements of Drop Size and Velocity Distributions," *Optical Engineering*, Vol. 23, No. 5, 1984, pp. 583–590.

[19]Hong, C. H., "Dynamic Characteristics of the Continuous and Dispersed Phases in a Hollow-Cone Spray," Ph.D. Dissertation, Inst. of Aeronautics and Astronautics, National Cheng-Kung Univ., Tainan, Taiwan, ROC, 1991.

[20]Crowe, C. T., Chung, J. N., and Troutt, T. R., "Particle Mixing in Free Shear Flows," *Progress in Energy and Combustion Science*, Vol. 14, No. 3, 1988, pp. 171–194.

[21]Durst, F., Milojevic, D., and Schonung, B., "Eulerian and Lagrangian Predictions of Particulate Two-Phase Flows: a Numerical Study," *Applied Mathematical Modeling*, Vol. 8, No. 2, 1984, pp. 101–115.

[22]Mostafa, A. A., and Mongia, H. C., "On the Modeling of Turbulent Evaporating Sprays: Eulerian Versus Lagrangian Approach," *International Journal of Heat and Mass Transfer*, Vol. 30, No. 12, 1987, pp. 2583–2593.

[23]Adeniji-Fashola, A., and Chen, C. P., "Modeling of Confined Turbulent Fluid-Particle Flows Using Eulerian and Lagrangian Schemes," *International Journal of Heat and Mass Transfer*, Vol. 33, No. 4, 1990, pp. 691–701.

[24]Shearer, A. J., Tamura, H., and Faeth, G. M., "Evolution of a Locally Homogeneous Flow Model of Spray Evaporation," *Journal of Energy*, Vol. 3, No. 5, 1979, pp. 271–278.

[25]Shang, H. M., Chen, C. P., and Jiang, Y., "Turbulence Modulation Effect on Evaporating Spray Characterization," AIAA Paper 90-2442, Orlando, FL, July 1990.

[26]Shuen, J-S., Soloman, A. S. P., Zhang, Q-F., and Faeth, G. M., "A Theoretical and Experimental Study of Turbulent Particle-Laden Jets," NASA CR-168293, Nov. 1983.

[27]Soo, S. L., *Fluid Dynamics of Multiphase System*, Blaisdell, Waltham, MA, 1967, Chap. 2, pp. 59–81.

[28]Putnam, A., "Integratable Form of Droplet Drag Coefficient," *ARS Journal*, Vol. 31, No. 10, 1961, pp. 1467–1468.

[29]Patankar, S. V., *Numerical Heat Transfer and Fluid Flow*, McGraw-Hill, New York, 1980, Chap. 5, pp. 79–100.

[30]Crowe, C. T., Sharma, M. P., and Stock, D. E., "The Particle-Source-In Cell Model for Gas-Droplet Flows," *Transactions of the ASME Journal of Fluids Engineering*, Vol. 99, No. 2, 1977, pp. 325–332.